Material Studies of Lipid Vesicles in the L_α and L_α-Gel Coexistence Regimes

Scott D. Shoemaker and T. Kyle Vanderlick
Department of Chemical Engineering, Princeton University, Princeton, New Jersey 08544 USA

ABSTRACT In this work, we utilize micropipette aspiration and fluorescence imaging to examine the material properties of lipid vesicles made from mixtures of palmitoyloleoylphosphocholine (POPC) and dipalmitoylphosphatidylcholine (DPPC). At elevated temperatures/low DPPC fractions, these lipids are in a miscible liquid crystalline (L_α) state, whereas at lower temperatures/higher DPPC fractions they phase-separate into L_α and gel phases. We show that the elastic modulus, K, and critical tension, τ_c, of L_α vesicles are independent of DPPC fraction. However, as the sample temperature is increased from 15°C to 45°C, we measure decreases in both K and τ_c of 20% and 50%, respectively. The elasticity change is likely driven by a change in interfacial tension. We describe the reduction in critical tension using a simple model of thermally activated membrane pores. Vesicles with two-phase coexistence exhibit material properties that differ from L_α vesicles including critical tensions that are 20–40% lower. Fluorescence imaging of phase coexistent POPC/DPPC vesicles shows that the DPPC-rich domains exist in an extended network structure that exhibits characteristics of a solid. This gel network explains many of the unusual material properties of two-phase membranes.

INTRODUCTION

The material properties of the cellular membrane are key to many biological processes. As the physical interface between the cell and the extracellular milieu, the lipid membrane regulates the permeation of molecules in and out of the cell, the mechanical response to environmental stresses, and, in the case of mechanosensitive membrane bound proteins, enzymatic activity. As a result, the material properties of cellular membranes and their synthetic derivatives, lipid vesicles, have been a subject of frequent study.

This paper focuses on the properties of lipid vesicles made from mixtures of palmitoyloleoylphosphocholine (POPC) and dipalmitoylphosphatidylcholine (DPPC). These lipids were chosen both for their biological relevance as well as their phase behavior. At elevated temperatures, the two components are fully miscible in the liquid crystalline (L_α) phase, whereas at reduced temperatures, they phase-separate into separate L_α and gel phases (Curatolo et al., 1985). This system thus allows systematic examination of the material properties of two-component lipid membranes both with and without phase separation.

Most studies on lipid vesicles have focused on the L_α phase because it is assumed to most closely resemble the behavior of real cellular membranes. Past work has demonstrated, for example, the role that surfactant intercalation (Evans et al., 1995; Needham and Zhelev, 1995), lipid composition (Olbrich et al., 2000; Rawicz et al., 2000), and surface charge (Shoemaker and Vanderlick, 2002a) plays in modulating the properties of L_α membranes. However, in the literature there is surprisingly little experimental work regarding the effects of temperature on the properties of membranes in this phase. This is despite the fact that, as self-assembled structures, membranes represent a careful balance of weak intermolecular forces and thus could be highly sensitive to moderate temperature changes. This is exemplified, for example, by the almost fourfold change in the bending modulus of phosphocholine membranes between 12°C and 34°C (Niggemann et al., 1995). The importance of temperature effects is also well-illustrated in nature by the example of *Lactobacillus acidophilus*. This organism changes its lipid membrane composition when grown at 25°C vs. 37°C, presumably to control membrane properties (Murga et al., 1999). In addition to gaining insight into biological phenomena, understanding how temperature affects lipid membrane mechanical properties is key to the successful use of vesicles for biotechnology applications. For example, vesicles used as drug delivery vehicles could experience large variations in temperature between processing, storage, and use.

Another topic of interest to the membrane community are the characteristics of phospholipid membranes with nonuniform composition. Evidence has accumulated in recent years that the composition of biological membranes can vary spatially in the plane of the membrane (Haverstick and Glaser, 1987; Rodgers and Glaser, 1991) and that these inhomogeneities play an important role in membrane function (Brown and London, 1998). The spatial compositional variance is likely driven by the phase separation of lipid mixtures (Schroeder et al., 1994), in which lipid species with sufficiently disparate gel transition temperatures exhibit equilibrium between gel domains rich in the higher melting temperature lipid and an L_α phase rich in the lower melting temperature lipid. Phase separation in lipid vesicles has been examined by a number of techniques such as DSC and NMR (Curatolo et al., 1985), electron microscopy (Hui, 1981), atomic force microscopy (Dufrene et al., 1997; Mou et al.,

Submitted July 26, 2002, and accepted for publication October 8, 2002.
Address reprint requests to T. Kyle Vanderlick, Tel.: 609-258-4891; Fax: 609-258-0211; E-mail: vandertk@princeton.edu.

0006-3495/03/02/998/12 $2.00

1995), and fluorescence methods (Bagatolli and Gratton, 2000a; Jorgensen et al., 2000; Korlach et al., 1999).

With a few notable exceptions, such studies concentrate on the presence, geometry, and formation rate of phase-separated lipid domains and provide little information on the material properties of the resulting two-phase bilayer. Clerc and Thompson demonstrated that two-component vesicles exhibit maximum permeation in the phase-separated regime and determined that solutes preferentially cross the bilayer at domain interfaces (Clerc and Thompson, 1995). Meleard et al. concluded that the unusually low bending moduli of vesicles made of erythrocyte lipid extract were due to phase coexistence (Meleard et al., 1997). However, studies elucidating the properties of either the individual domains or of the two-phase membrane as a whole remain scarce.

In this paper, we report on the temperature and compositional dependence of the material properties of mixed POPC/DPPC membranes, both in the single (L_α) and the two-phase (L_α-gel) state. Our results show that the area stretch elasticity, K, and tension required to rupture, τ_c, of L_α phase bilayers are independent of composition but decrease with increasing temperature. For vesicles in the two-phase coexistence regime, we find markedly altered mechanical characteristics, including nonelastic behavior and reductions in τ_c of 20–40%. Using fluorescence microscopy, we show that the changes in mechanical properties coincide with the formation of a network of long, thin gel-like domains in the L_α vesicle matrix. These fluorescence observations aid in the explanation of the unusual mechanical behavior of phase-separated lipid vesicles.

METHODS

Reagents

POPC, DPPC, and rhodamine-labeled dioleoylphosphatidylethanolamine (Rh-PE) were purchased from Avanti Polar Lipids (Alabaster, AL) and stored at −8°C as ~0.5 mg/ml chloroform solutions. The exact lipid concentration was determined using a spectrophotometric assay described by Avanti. Unless otherwise stated, all other chemicals were from Sigma (St. Louis, MO), of the highest grade available, and used as received. Water used was produced by a Milli-Q UF unit (Millipore, Bedford, MA) and had a resistivity of 18.2 Megohm-cm.

Vesicle preparation

Giant unilamellar vesicles (GUVs) for both micropipette aspiration and fluorescence imaging were created using a modification of the electroformation method (Angelova and Dimitrov, 1987; Longo et al., 1997). POPC and DPPC were combined at the desired ratio; vesicles for fluorescence imaging were additionally doped with 0.4%–2% Rh-PE. 50 μl of the lipid solution was spread on platinum electrodes in a Teflon/glass cell. Films were dried under vacuum overnight to remove trace solvent. 150 mM sucrose solution was added to the chamber as vesicle interior solution. It has been shown that GUV formation requires incubation above T_g, the lipid's gel transition temperature (Needham and Evans, 1988). Similarly, for mixtures we found that temperatures above the single highest transition temperature (in this case, DPPCs, with $T_g \sim 41$°C (Silvius, 1982)) were needed to create vesicles with the desired composition. Therefore, the interior solution was preheated and electroformation process was run at 50°C. Vesicles formed under the action of a 1.5-V sine wave operating at 10 Hz for 15 min, then 3 Hz, 1 Hz, and 0.5 Hz for 5 min each. After formation, vesicles were stored at room temperature and used within 8 h of preparation. When creating fluorescent vesicles, samples were kept covered at all times to minimize photobleaching.

Micropipette aspiration

We used the micropipette technique to determine the area dilational elasticity and critical tension of vesicles made from POPC/DPPC mixtures. The temperature and composition of vesicles was modulated to explore both the single L_α phase and the L_α-gel coexistence region. A more complete description of our experimental method has been given previously (Shoemaker and Vanderlick, 2002b). We note only the changes in procedure here.

Just before micromanipulation, GUVs were mixed with a glucose exterior solution and equilibrated at the desired temperature for at least 20 min. The glucose concentration of the exterior solution ranged from 130 mM (used with 45°C studies) to 165 mM (used with 15°C studies). Glucose concentration was chosen such that the vesicles would slightly deflate, giving them ~5% excess membrane area to aid in micropipette aspiration (both lipids and solutions change volume/area with temperature, necessitating different gradients). Vesicles were then added to a glass/teflon observation chamber whose temperature was held constant by a circulating bath. Samples were allowed an additional 5 min to equilibrate before manipulation. As a result, over the course of a common experiment individual vesicles were held at temperature for 30–90 min before examination. In agreement with other groups (de Almeida et al., 2002; Jorgensen et al., 2000), it was observed that although domains initially form very rapidly, the timescale for complete equilibration is a few hours. This means that our experimental samples were to some degree still evolving. In response, we note that measurements are invariant over the experimental time range (~1 h), suggesting the total maturation of domains does not greatly alter vesicle material properties.

For examination, vesicles with diameters of 25–40 μm were selected with a glass microcapillary having an internal diameter of ~6 μm. Vesicles were prestressed by application of a 3-in water suction pressure then returned to a low-pressure state (< 0.2 in of water). A kdScientific syringe pump (New Hope, PA), previously calibrated with Validyne pressure transducers (Advanced Controls, Warminster, PA), increased the applied suction pressure at a constant rate of 0.1 mN/m/s. This process was observed using an inverted microscope fitted with differential interference contrast and fluorescence optics (Nikon TE200, Micron Optics, Cedar Knoll, NJ) and recorded using a Kodak ES310 CCD camera connected to a PC via a PIXCI-D imaging board (EPIX, Buffalo Grove, IL).

Micropipette aspiration induces membrane tensions due to the Laplace pressure jump across curved interfaces. This is embodied in the equation

$$P_{in} - P_{out} = \frac{2\tau}{R}, \tag{1}$$

where P_{in} and P_{out} are the inside and outside pressures, respectively, τ is the induced tension, and R is the local radius of curvature. For micropipette analysis, this equation is applied to both the portion of the vesicle inside and outside the pipette, resulting in (Evans and Needham, 1987)

$$\tau = \frac{\Delta P \times R_p}{2\left(1 - \frac{R_p}{R_o}\right)}, \tag{2}$$

in which ΔP is the applied suction pressure, R_p is the pipette radius, and R_o is the vesicle radius. The resulting membrane strain, α, can be found using (Evans and Needham, 1987)

$$\alpha \simeq \frac{2\pi R_p \Delta L}{A_o}\left(1 - \frac{R_p}{R_o}\right), \quad (3)$$

where ΔL is the change in vesicle projection length and A_o is the total membrane area measured at the initial low-pressure state. ΔL, R_p, and R_o were measured optically using the Subpixel Edger tool in the XCAP software package (EPIX, Buffalo Grove, IL).

Following typical micropipette aspiration protocol, the area stretch elasticity modulus, K, was determined as the slope of the applied tension versus the areal strain above $\tau = 0.5$ mN/m. In some cases, particularly at elevated temperatures, the stress/strain function curved downward slightly instead of showing the completely linear response expected for an elastic material. This behavior coincided with a small but measurable hysteresis when applied stress was reduced, suggesting that the deviation was due to increased solute permeation and/or evaporation and not nonelastic membrane response. In these cases, only the straight portion of the curve was fit. The critical tension was defined as the last recorded tension before membrane rupture. All measurements were performed at a constant pulling rate of 0.1 mN/m/s. Approximately 10 vesicles were examined at each temperature/composition and the results are presented as average ± SD.

Fluorescence imaging

Except for being labeled with the fluorescent tag Rh-PE, vesicles observed by fluorescence microscopy were identical to those examined by micropipette analysis. The same microscope, camera, and software package described above were used in the collection and analysis of images. Filter cubes with excitation wavelengths of 510–560 nm and emission cutoff of 590 nm were used. Unless otherwise noted, vesicles were equilibrated at the desired temperature for at least 20 min and then placed on the microscope stage for observation. Temperature was monitored by a thermocouple inserted into the sample cell. The image focal plane was either the top or the bottom of the vesicle under observation. Other experimental details were identical to those described above.

RESULTS AND DISCUSSION

In this work, we use micropipette aspiration and fluorescence techniques to determine the material properties of lipid vesicles as a function of lipid composition and temperature. The lipids utilized were POPC and DPPC, which are lipids common to mammalian cell membranes (Yeagle, 1992) and the surfactant lining of the lung (Veldhuizen et al., 1998), respectively. POPC (16:0, 18:1) and DPPC (16:0, 16:0) are structurally closely related, differing only by two methylene groups and a single unsaturated bond in one of the carbon tails. The main gel transition temperatures are quite different, however, at −2°C and 41°C, respectively (Silvius, 1982). This difference is sufficient to cause bulk phase separation in lipid membranes. The phase diagram of this system was first measured by Curatolo et al. using DSC (Curatolo et al., 1985) and is redrawn in Fig. 1. As demonstrated in the figure, at high temperatures the system is in a single liquid crystalline (L_α) phase. At intermediate temperatures, there is a large L_α-gel coexistence region and at lower temperatures the system exhibits gel-gel immiscibility (Curatolo et al., 1985).

Our observations of this system will be described in three separate sections. The first deals with the mechanical properties of L_α phase lipid vesicles. Next, we will describe the mechanics of vesicles within the two-phase L_α-gel coexistence region. Finally, we will describe fluorescence imaging of POPC/DPPC vesicles, the physical properties of the gel domains, and how these domains influence the mechanical properties of two-phase lipid membranes.

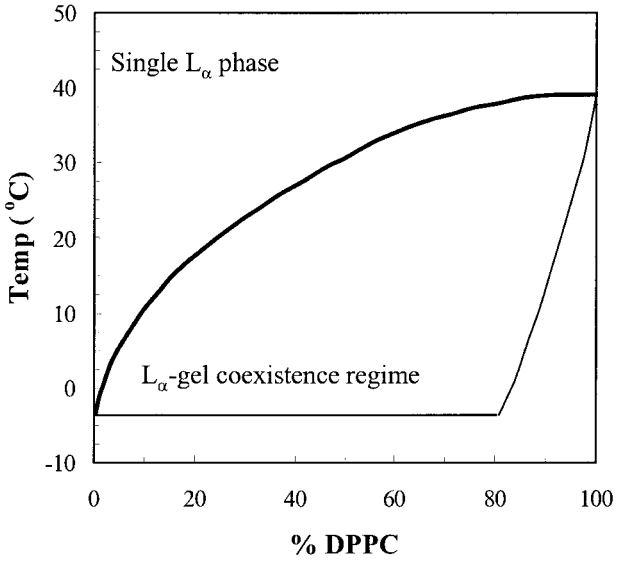

FIGURE 1 L_α and L_α-gel regions of the phase diagram for the POPC/DPPC system (redrawn from Curatolo et al. (1985)). The darkened line is referred to in the text as the coexistence line.

Mechanical characterization of L_α phase POPC/DPPC mixtures

Regardless of composition and temperature, vesicles examined above the coexistence line shown in Fig. 1 appeared fluid. Flaccid vesicles appeared spherical with mild, isotropic fluctuations, as shown in Fig. 2 *A*. Stress-strain curves were similar to curves typically found for the L_α phase. As typified in Fig. 3 *A*, curves were linear and nonhysteretic on aspiration and release.

Fig. 4 shows the results of membrane stretch elasticity tests for L_α phase vesicles as a function of composition and temperature. These values are in the range normally seen for lipid vesicles and agree with our previous value for POPC (Shoemaker and Vanderlick, 2002b). There is no clear compositional dependence seen. This qualitatively agrees with the work of Rawicz et al. who showed little effect of monounsaturated bonds on vesicle elasticity (Rawicz et al., 2000).

Fig. 4 demonstrates that regardless of composition, membrane elasticity decreases ~40 mN/m (a 20% reduction) as temperature is increased from 15°C to 45°C. For comparison, Kwok and Evans measured the thermal area expansivity of eggPC bilayers as $2.4 \times 10^{-3}\ K^{-1}$ (Kwok and Evans, 1981). This change in molecular area can be related to surface

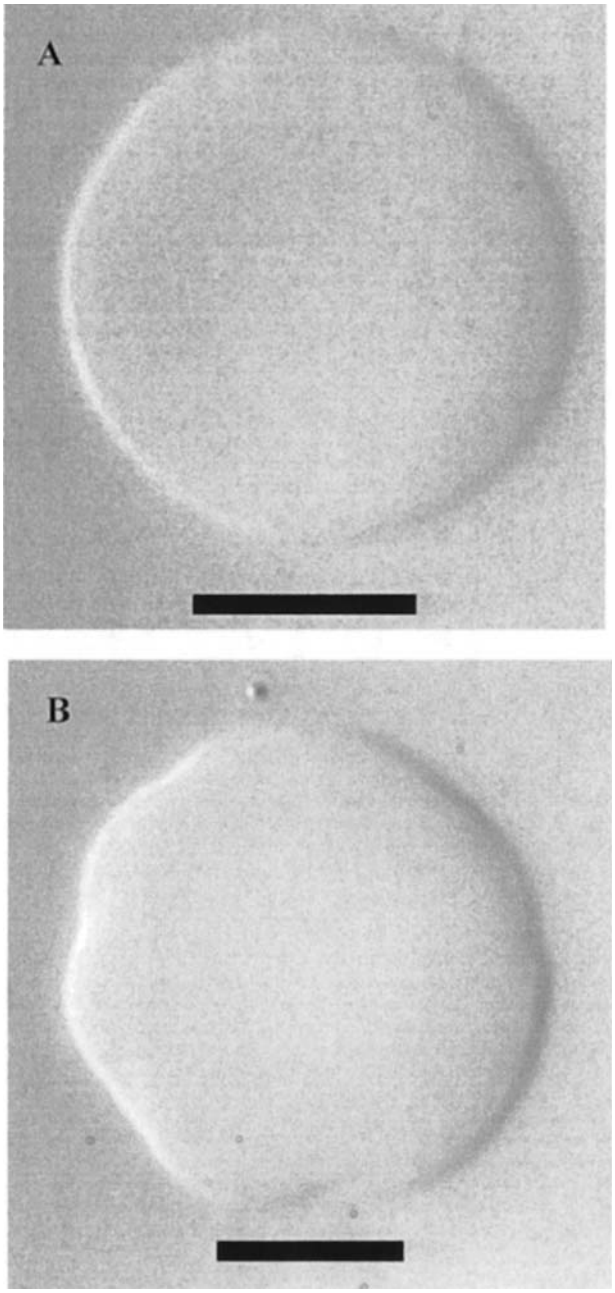

FIGURE 2 POPC/DPPC vesicles observed with differential interference contrast optics. (*A*) A L_α phase vesicle (80% POPC, 25°C) appears round with small perturbations due to thermal fluctuations. (*B*) A two-phase vesicle (80% POPC, 15°C) is nonspherical and fluctuates little. Scale bars represent 10 μm. Image contrast enhanced using XCAP image analysis software.

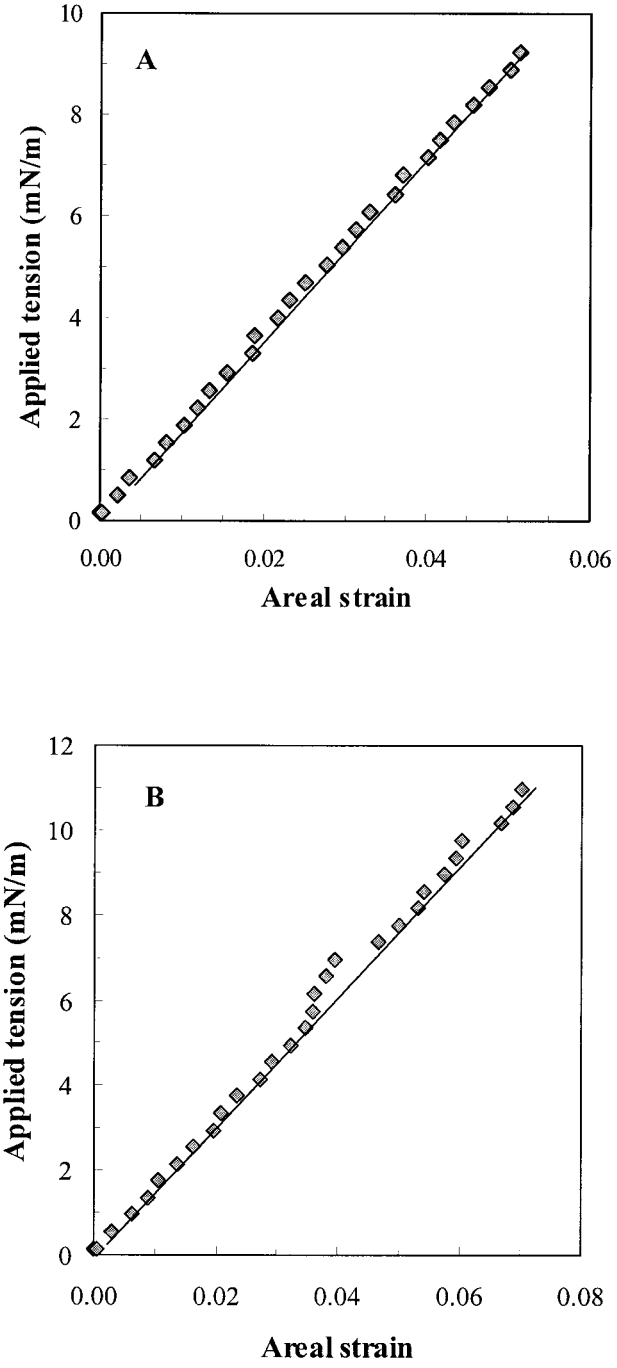

FIGURE 3 Representative stress/strain plots for 53.2% POPC/46.8% DPPC vesicles at (*A*) 35°C (L_α phase), and (*B*) 25°C (two-phase coexistence). Lines are drawn to guide the eye.

pressure, and thus elasticity, by a two-dimensional van der Waals model of the bilayer (Evans and Skalak, 1980). This methodology predicts a 23 mN/m decrease in K as temperature increases from 15°C to 45°C, somewhat less than our measured effect. The disagreement may be due in part to the effect of temperature on bending elasticity. Following common micropipette convention, we have calculated elasticity as the slope of the stress/strain curve at high (greater than 0.5 mN/m) tensions. However, it has recently been pointed out that in this high tension regime, the bending modulus plays a small role in stress/strain behavior due to the smoothing of residual thermal fluctuations (Rawicz et al., 2000). Thus, temperature effects on the bending modulus could influence measured values of areal stretch elasticity. Using the temperature-dependent bending

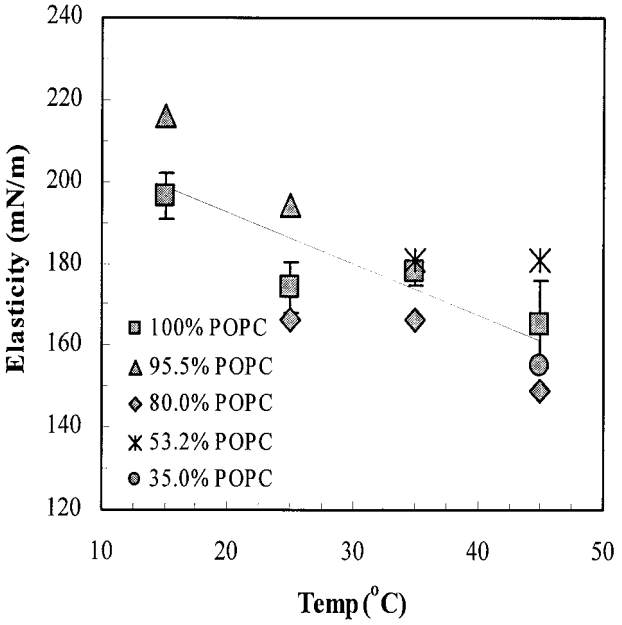

FIGURE 4 Membrane dilational elasticity measurements for POPC/DPPC vesicles in the L_α phase. Error bars shown for 100% POPC (average ± SD) are representative of all measurements. The solid line is the least-squares fit of all data.

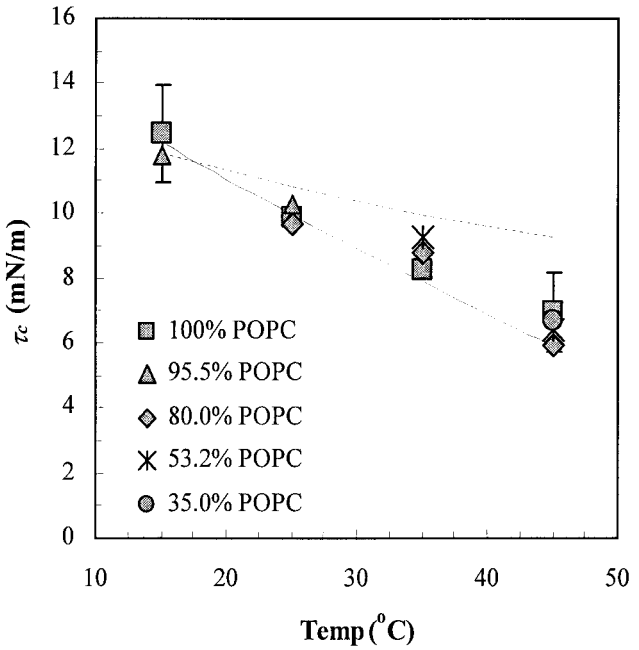

FIGURE 5 Measured critical tensions for POPC/DPPC vesicles in the L_α phase. Error bars shown for 100% POPC (average ± SD) are representative of all measurements. The solid line represents the results of Eq. 5 and the dotted line is the prediction from solving Eqs. 6–8.

moduli for membranes of DMPC (Fernandez-Puente et al., 1994) or DOPC (Niggemann et al., 1995) estimates are that the apparent areal dilation elasticity (i.e., the linear fit from the high tension regime) will decrease by 3 mN/m or 21 mN/m, respectively, between 15°C and 45°C simply due to the change in bending elasticity. The measured reduction in dilational elasticity thus represents the sum of bending and dilational elastic moduli effects.

Another approach to the temperature effect on K is based on the Isrealachvili-Mitchel-Ninham (IMN) model of lipid membranes (Israelachvili et al., 1980). In this framework, the attractive interfacial tension of the lipid film, γ, is balanced by a repulsive term dominated by steric and electrostatic interactions. Taking small perturbations from the equilibrium area per lipid molecule gives the simple relation $K = 4\gamma$ (Israelachvili et al., 1980). Thus any temperature dependence of the interfacial tension will result in a change in area elasticity. To quantify this effect, we will use the temperature dependence of interfacial tension found for linear hydrocarbons of ~0.05–0.1 mN/m/°C (Jasper and Duncan, 1967; Washburn, 1927). This results in a predicted elasticity effect of ~0.2–0.4 mN/m/°C, somewhat smaller than the dependence measured of 1.2 mN/m/°C. This again may be due to bending modulus effects.

Shown in Fig. 5 is the compositional and temperature dependence of the critical tension, τ_c, for vesicles in the single L_α phase regime. We note that the value found for 100% POPC vesicles at 25°C, 9.9 ± 2.5 mN/m, is significantly higher than our previously published value of 6.5 ± 1.4 mN/m (Shoemaker and Vanderlick, 2002b). This is because measured critical tension increases with increasing pulling rate (Evans and Ludwig, 2000) and the present work utilized a much faster rate (0.1 vs. 0.015 mN/m/s). We found remarkable agreement between different compositions at the same temperature, indicating that POPC/DPPC composition again does not influence vesicle mechanical properties. This qualitatively agrees with work by Olbrich et al. who showed the critical tension of single-component vesicles formed with different monounsaturated chains was similar (Olbrich et al., 2000).

Fig. 5 shows that there is a clear temperature dependence, as, independent of composition, membrane critical tension decreases by almost 50% as the temperature is increased from 15°C to 45°C. There are three obvious rationales for this reduction: a chemical degradation of the lipid molecules at elevated temperatures, an increase in available thermal energy to activate membrane breakdown, or a change in a temperature dependent membrane property (thus mirroring the interfacial tension effect described above). Lipids are hydrolyzed in aqueous solutions, a reaction aided by increased temperatures. This explains, for example, the marked reductions we measure for both K and τ_c for lipid membranes stored in a 50°C oven overnight (unpublished data). However, over the course of an ~1 h experiment, we do not measure any change in vesicle properties, suggesting little in situ lipid alteration. Moreover, POPC vesicles formed and examined at 25°C show identical mechanical properties to

ones formed at 50°C then cooled to 25°C (data not shown). This suggests that negligible lipid breakdown occurs on the timescale of vesicle production, again ~1 h, and more importantly, demonstrates that the temperature effect is reversible. We therefore conclude the critical tension reduction cannot be due to lipid degradation.

We believe it likely that the marked reduction in critical tension is due primarily to the increase in thermal energy available to the bilayer. Membranes are believed to break down via an activated process in which pores, which represent a balance between membrane tension τ and line tension ε, reach an energetically unstable size (Deryagin and Gutop, 1962). This indicates that membranes at a higher temperature have a greater chance of activating an unstable pore, even if all other membrane characteristics are identical.

To quantify this possibility, we consider the energy of a critical pore, E_{pore}, which is given as $\pi\varepsilon^2/\tau$ (Needham and Nunn, 1990). One would predict that a bilayer ruptures when E_{pore} approaches the available thermal energy, giving the critical tension as

$$\tau_c = \frac{\pi\varepsilon^2}{k_B T}, \tag{4}$$

where k_B is Boltzmann's constant and T is temperature. However, critical tensions measured by micropipette are commonly only a few percent of $k_B T$. This is due at least in part to the fact that Eq. 4 is valid for extremely rapid pulling rates; experimentally relevant rates produce critical tensions that are much lower (Evans and Ludwig, 2000). Because all of our measurements were completed at a constant pulling rate, we can to first approximation avoid this difficulty by examining changes in τ_c rather than absolute values. Taking the derivative of Eq. 4 and assuming $\varepsilon \neq f(T)$ gives

$$\frac{\partial\tau_c}{\partial T} = -\frac{\pi\varepsilon^2}{k_B T^2}. \tag{5}$$

The expected change in critical tension due to the increase in thermal energy is computed and shown by the solid line in Fig. 5 using the edge energy given by Zhelev and Needham for the structural intermediate of POPC and DPPC, stearoyloleoylphosphatidylcholine (18:0, 18:1 PC) (Zhelev and Needham, 1993). There is surprisingly good agreement with the measured data. Although noting that this is to a small degree fortuitous due to the sensitivity of the agreement to the value of ε used, clearly the basic hypothesis is supported.

An intriguing result falls out of Eq. 5 when the function is extrapolated to higher temperatures. The predicted critical tension reaches zero near 80°C, suggesting that simple phosphatidylcholine membranes become unstable and spontaneously rupture around this temperature when faced with the slightest stress. Although this is well above physiological conditions for most organisms, a number of thermophilic archaebacteria thrive at this temperature. One might speculate that avoiding this spontaneous thermal rupture is one of the reasons for the unique molecular architecture found in archaebacterial lipids (Kates, 1993).

An alternative approach to examining the reduction in critical tension through higher available thermal energy can be performed using the recent results of Evans and Ludwig (Evans and Ludwig, 2000). By combining Kramers' theory for reaction kinetics and classical nucleation theory, these authors showed a universal relationship for critical tension in the form of

$$\frac{\tau_\beta}{\tau_c} \approx \frac{5}{2}\ln\left(\frac{\tau_c}{\tau_\beta}\right) - \ln\left(\frac{r}{r_\beta}\right), \tag{6}$$

where r is the pulling rate, and τ_β, the thermal tension, and r_β, the thermal loading rate, are defined as

$$\tau_\beta = \frac{\pi\varepsilon^2}{k_B T} \tag{7}$$

$$r_\beta \sim \frac{\tau_\beta \varepsilon^2 D}{(k_B T)^2}\exp\left(\frac{-E^o}{k_B T}\right), \tag{8}$$

where D is lipid diffusivity and E^o is the barrier to hole formation. With this formulation, knowledge of D, E^o, and ε allows the qualitative prediction of the temperature dependence of τ_c. We use the results of Evans and Ludwig for the lipid SOPC (18:0, 18:1) (Evans and Ludwig, 2000) to estimate the parameters ε and E^o (assuming these properties to be temperature invariant) and work by Vaz et al. (1985) for temperature-dependent values for POPC diffusivity. The resulting prediction is shown by the dotted line in Fig. 5. The general monotonic decreasing trend is again captured, but the predicted effect is ~50% less than either the experimentally measured effect or the effect predicted from Eq. 5, likely due to the errors in estimating E^o from literature data. However, the prediction of a large decreasing trend is still captured, suggesting that an increase in thermal energy is indeed the likely culprit for the measured reduction in τ_c with increasing temperature.

Finally, we note that we cannot dismiss our third proposed reason for the critical tension reduction, which was a temperature-dependent change in membrane characteristics. Using the above formalism, a reduction in τ_c could derive from a reduction in line tension with increasing temperature. Unfortunately, we do not know of any studies that have characterized a possible temperature effect on ε. However, the agreement between our data and the thermal energy models suggests that any change in membrane properties such as ε is likely secondary in effect.

Mechanical characterization of two-phase POPC/DPPC mixtures

Lipid vesicles were examined below the two-phase coexistence line as a function of composition and temperature. Figs. 2 and 6 show micrographs of representative lipid

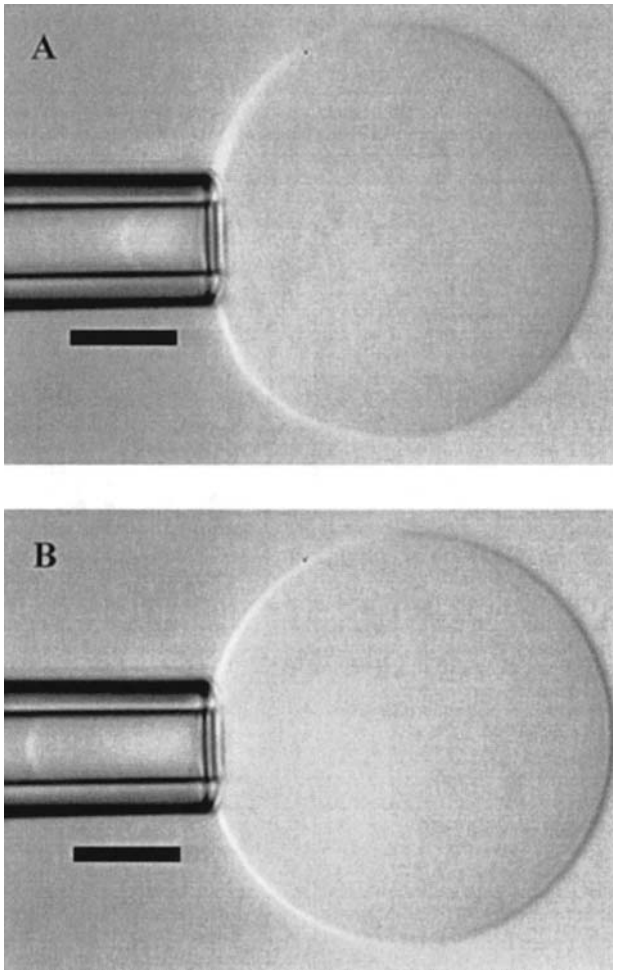

FIGURE 6 DIC images of the same two-phase vesicle (20% POPC, 25°C) under ~0.05 mN/m tension, both before (*A*) and after (*B*) prestressing. Note that the vesicle is initially somewhat oblate (*A*), but after prestressing the vesicle is completely spherical (*B*). Because both images are at the same tension, the change in projection length is the result of smoothing out the initially rough topology. Scale bars represent 10 μm. Image contrast enhanced using XCAP image analysis software.

vesicles above and below the coexistence line taken with differential interference contrast optics. Evidence of L_α-gel coexistence could be seen simply by optical microscopy. Instead of fluctuating isotropically about a sphere like a fluid vesicle (Fig. 2 *A*), two-phase vesicles frequently had irregular surface topology and showed little fluctuation (Fig. 2 *B*). At large DPPC fractions, this irregular topology occasionally continued even when aspirated by the micropipette at low (~0.05 mN/m) tension (see Fig. 6 *A*). However, after prestressing the vesicle and returning to low tension, vesicles always appeared to adopt an overall spherical shape (see Fig. 6 *B*).

Although irregular vesicle shapes were noted in one previous report (Meleard et al., 1997), studies usually are not able to detect phase coexistence with optical microscopy. From Fig. 6 we see that the irregular surface topology requires excess membrane area (that is, for the vesicles to be partially deflated). As mentioned in the Methods section, we slightly deflate vesicles with an osmotic gradient before mechanical characterization to assist in aspiration. It is this deflation that allows us to see nonspherical structures like the one seen in Fig. 2 *B*.

As suggested in Fig. 6, stress/strain curves measured using two-phase vesicles differed from curves measured for fully L_α membranes (a representative stress/strain curve for a L_α vesicle is shown in Fig. 3 *A*). The deviation from purely elastic behavior—defined here as linear stress/strain curves with no hysteresis—increased the further vesicles were from the coexistence line. Near the single-phase region, vesicles often had stress/strain curves that were predominately straight with ''steps'' superimposed (see Fig. 3 *B*). Deeper into the two-phase region, curves were highly nonlinear and showed great hysteresis (see Fig. 7). Thus the mechanical behavior of two-phase membranes differs markedly from that of fully L_α phase vesicles, which are described by an area stretch elasticity (i.e., Fig. 3 *A*), and fully gel-phase vesicles, which are best identified by yield shear and shear viscosity under plastic flow (Evans and Needham, 1987). Attempts to characterize phase coexistence membranes with these measures failed to give consistent and meaningful results and are not reported here.

Vesicle critical tension, on the other hand, was found to be fairly consistent from vesicle to vesicle. Although one must be cautious using Eq. 2 to calculate τ_c for these two-phase membranes (see below), interesting trends emerge when

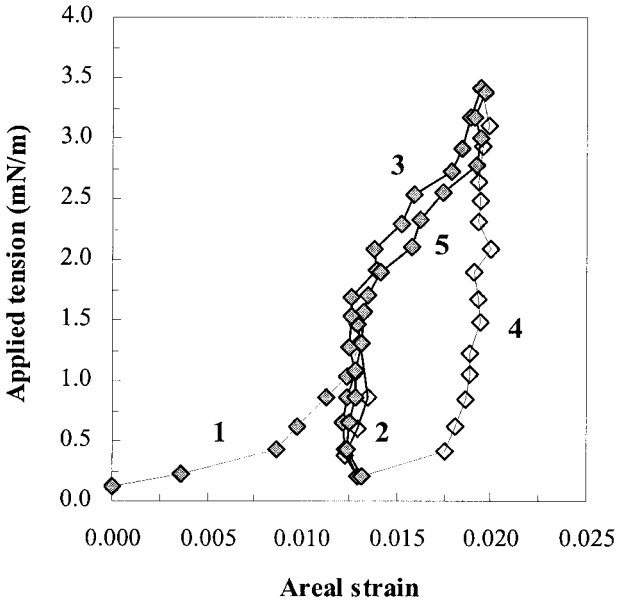

FIGURE 7 Stress history of a 20% POPC/80% DPPC vesicle at 25°C. The applied tension was increased (*filled symbols*) then decreases (*open symbols*) repeatedly. Numbers shown on the plot indicate the order of events. The large initial deformation (compare to the total strains seen in Fig. 5) smoothes out the vesicle to a sphere.

comparing the critical tensions of two-phase vesicles with their single L_α phase counterparts. Data from both single- and two-phase membranes are shown in Fig. 8. To remove the temperature dependence discussed earlier, data are normalized by the critical tension of L_α phase vesicles at that temperature. We refer to this normalized quantity as reduced critical tension. Also plotted on the figure as dotted lines are the DPPC fractions at which the vesicles cross from the single L_α phase to the two-phase coexistence region (note Fig. 8 *D* is above the gel transition temperature of DPPC meaning vesicles are always in the L_α phase). As seen in the figure, data points on the left on the coexistence line are all ~1.0, indicating L_α phase behavior, whereas points to the right range between 0.6 and 0.8, indicating a reduction of critical tension for two-phase lipid vesicles of 20–40%. The data are replotted in Fig. 9 as reduced critical tension versus the fraction of lipid membrane in the gel phase (calculated using the phase diagram in Fig. 1). It is possible that there is a small increase in stability with gel fraction, but within the experimental error of the measurement all coexistence vesicles appear to have identical reduced critical tensions of ~0.75.

Fluorescence imaging of two-phase coexistence

To gain insight into the behavior of vesicles showing L_α-gel coexistence, POPC/DPPC vesicles doped with Rh-PE were imaged by fluorescence microscopy. When imaged above the coexistence line, vesicles appeared homogeneous, implying a single phase (see Fig. 10, *top*). Marked changes in vesicle appearance were seen upon cooling into the two-phase coexistence region. Images were no longer homogeneous as there were clear light and dark regions in the membrane. The temperature at which the dark domains first appeared approximately corresponded with the coexistence

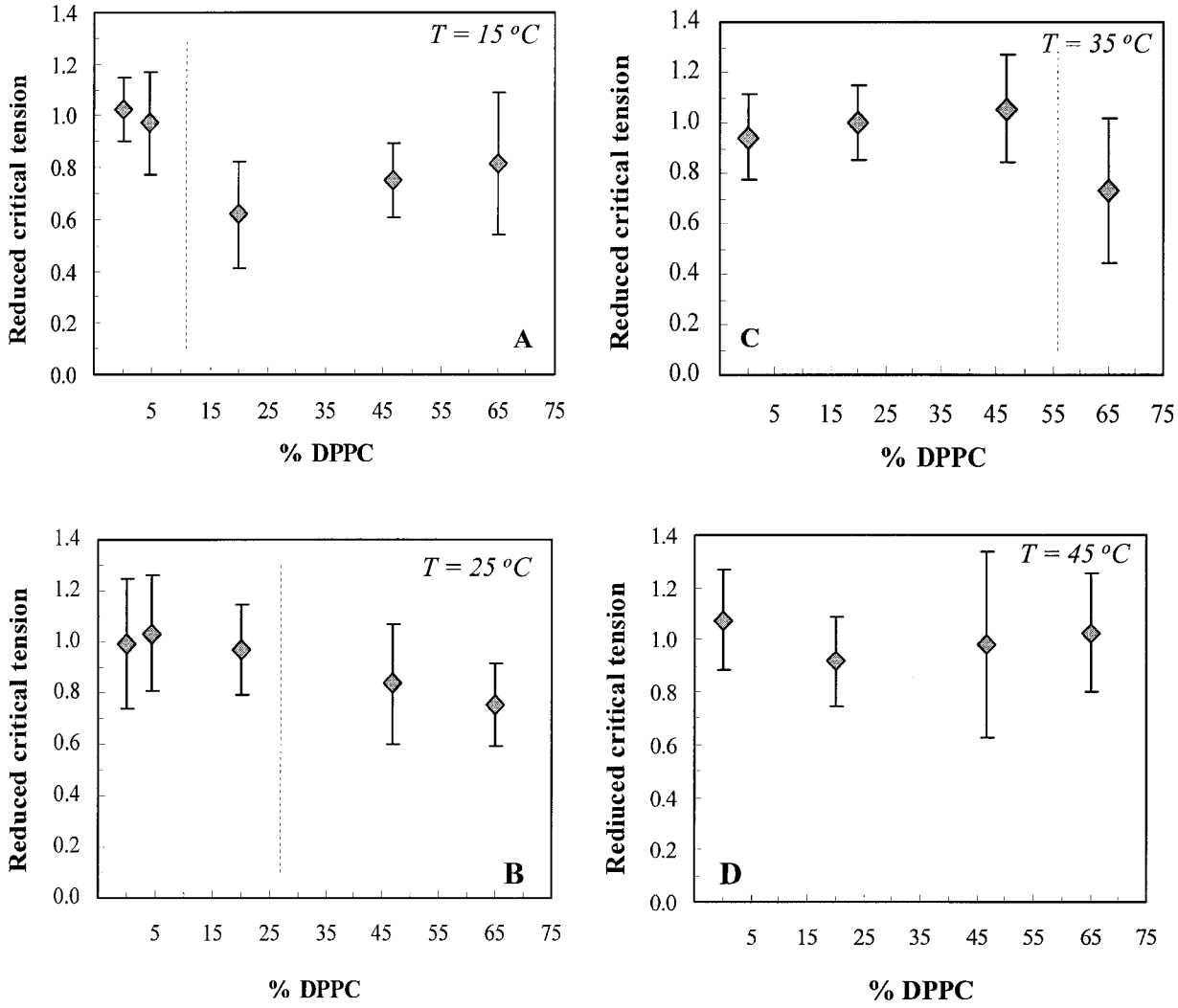

FIGURE 8 Reduced critical tensions of POPC/DPPC vesicles as a function of composition at (*A*) 15°C, (*B*) 25°C, (*C*) 35°C, and (*D*) 45°C. Dashed lines represent the composition at which the lipid mixture phase separates based on the phase diagram shown in Fig. 1. Data plotted as average ± SD.

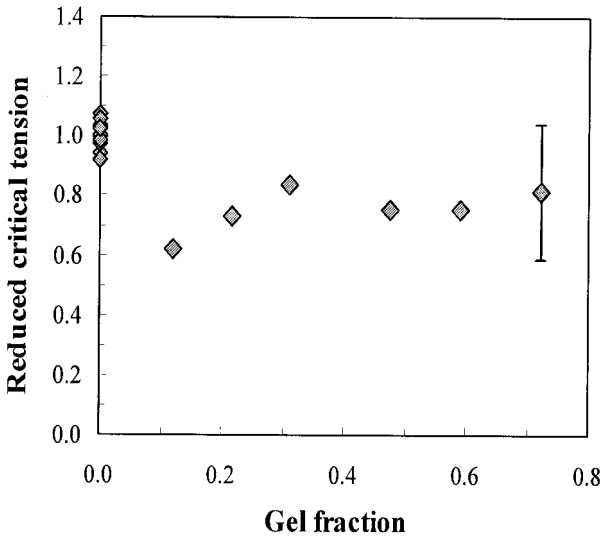

FIGURE 9 Reduced critical tension as a function of the fraction of lipid in the gel state. Gel fractions calculated using the lever rule and the phase diagram shown in Fig. 1.

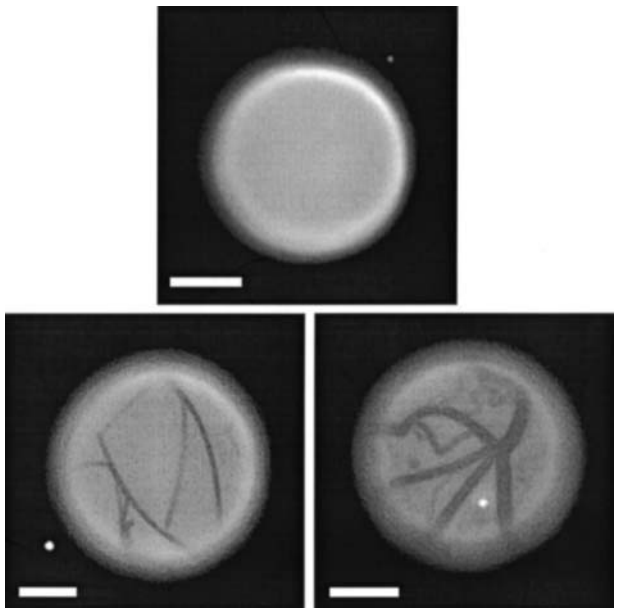

FIGURE 10 Representative fluorescence images of 40% POPC/59% DPPC/1% Rh-PE vesicles. (*Top*) A L_α phase vesicle at 39.4°C appears completely homogeneous. (*Bottom left*) A vesicle at 22.6°C, just under the coexistence line, shows a few long, thin domains that already have a network configuration. (*Bottom right*) After further reducing the sample temperature to 16.2°C, domains grow in thickness. Scale bars represent 10 μm. Image contrast enhanced using XCAP image analysis software.

line shown in Fig. 1 (Curatolo et al., 1985). Fig. 10 bottom left shows a representative image of vesicles within the L_α-gel coexistence regime but near the phase boundary. A few long, thin, dark lines are seen against a bright background. Even at very low surface coverage, these thin lines appear to form a network in the lipid membrane. As shown in Fig. 10 bottom right, further cooling of the vesicles results in growth of domains. Unfortunately, reproducible quantification of domain fraction was impossible.

Vesicle images were always binary, meaning areas were either dark or light. The lack of areas of intermediate brightness indicates that domains are superimposed in both of the membrane's monolayers and suggests strong coupling between the two molecular sheets (Bagatolli and Gratton, 2000b; Korlach et al., 1999). Vesicles from the same sample were not perfectly homogeneous in domain width or surface coverage. In particular, it appeared that smaller vesicles on average had wider domains than larger vesicles. This may indicate that membrane curvature plays a role in nucleation and domain formation. However, the general shape of the features—long, thin, fairly straight interconnected segments—was constant regardless of the lipid composition or temperature of the sample provided they reside within the two-phase regime and sufficient time (i.e., more than a few minutes) was allowed for domain ripening. It is unlikely that the presence of the probe controlled domain formation or shape, as domain features did not depend on tag concentration over the range tested (0.4 mol%–2.0 mol%).

Fig. 10 represents the first direct visualization of freestanding bilayer phase coexistence using an unsaturated lipid (i.e., POPC). The domain shapes are significantly different than those imaged in a POPC/DPPC bilayer on a mica substrate using atomic force microscopy (Mou et al., 1995), suggesting domains are sensitive to preparation technique and/or the presence of a substrate. Similar domains, however, have been seen in freestanding bilayers made of DPPC and the saturated lipid dilauroylphosphatidylcholine (DLPC, 12:0, 12:0 PC) (Bagatolli and Gratton, 2000a; Korlach et al., 1999). Bagatolli and Gratton have examined various saturated lipid mixtures and describe the resulting domain shapes based on the difference in the hydrocarbon length of the two phospholipid molecules (Bagatolli and Gratton, 2000a). Noting that the gel transition temperatures for POPC (−2°C) and DLPC (−1°C) are approximately equal, our results suggest that this quantity is a more general criterion for the prediction of lipid domain shape inside the phosphocholine family. This finding is applicable to Monte Carlo simulations of binary phase separations as well, because past work has utilized the difference in chain length as the ''universal interaction parameter'' (Jorgensen et al., 1993).

The domains described in this work appear dark because the unsaturated chains of the fluorescent tag are locally excluded; this strongly suggests the domains are a tightly packed gel phase (Bagatolli and Gratton, 2000b). However, until now, one of the defining characteristics of a gel phase—rigidity—has not been clearly demonstrated in a two-phase bilayer. Fig. 11 shows various examples of solid-like behavior of the domains, confirming their gel nature. A flaccid two-phase vesicle with nonspherical cross section is

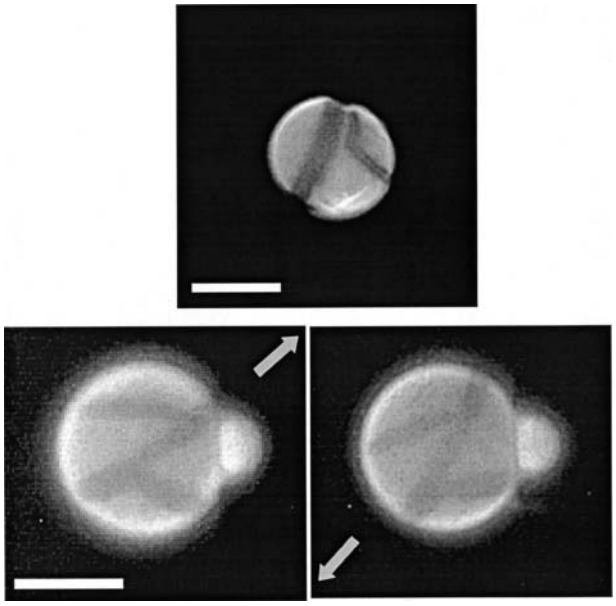

FIGURE 11 Fluorescence images of 40% POPC/60% DPPC vesicles in the two-phase regime. (*Top*) Vesicle at 16.8°C (1 mol% Rh-PE tag) whose nonspherical topology is caused by gel domains. (*Bottom left* and *right*) Vesicle at 24.2°C (0.5 mol % Rh-PE tag) held under light aspiration. Fluid flow is imposed in the direction of the arrows shown. In (*bottom left*), imposed flow has rotated the network until it hits the top of the pipette tip. In (*bottom right*), imposed flow has been reversed and the vesicle rotates ~30° until the network hits the bottom of the pipette tip. Scale bars represent 10 μm. Image contrast enhanced using XCAP image analysis software.

shown in Fig. 11 top. The figure shows domains aligned with the deformations, suggesting that they are a rigid support skeleton in an otherwise fluid membrane. Fig. 11, bottom left and right, shows a two-phase vesicle near the coexistence line lightly held by a micropipette tip in an alternating flow field. The fluid nature of L_α vesicles allows them to freely rotate when in a nonaxial flow field, even when held by slight aspiration (data not shown). When a vesicle with an extensive domain network is aspirated under flow, no rotation is possible (data not shown). This is because the vesicle is held by its rigid domain network, restricting motion. The vesicle in Fig. 11, bottom left and right, is being held by a portion of the membrane without visible domains, meaning a L_α region of the surface. As the vesicle is subjected to alternating flows (in the picture, flows toward the two arrows shown), the vesicle rotates ~30° but is stopped when the domain network comes in contact with the micropipette. A finite bending rigidity stops the domains from entering the pipette and adopting the resulting high radius of curvature.

Fluorescent observation of coexistent vesicles explains much of the unusual behavior noted in the previous section. Figs. 10 and 11 show that the size of the rigid domains is on order of the vesicle radius. This, combined with the network configuration described above, is what causes two-phase vesicles to adopt nonspherical topology as seen in Figs. 2 *B* and 11, top. If, for example, gel-phase lipid was distributed only in small islands rather than an extended network, domains could not cause the unusual vesicle shapes reported here. We should note that our observations do not preclude the existence of nanoscopic domains such as those seen by electron spin resonance (Sankaram et al., 1992) and infrared spectroscopy (Mendelsohn et al., 1995), as the minimum resolution of fluorescence microscopy is ~0.5 μm. However, such aggregates clearly could not contribute to the nonspherical vesicle topologies reported.

A network of gel domains also aids in the explanation of the nonlinear stress/strain behavior seen with phase coexistence vesicles. L_α phase membranes possess zero surface rigidity; this is well demonstrated in experiments that analyze the thermal fluctuations of vesicles to probe bending moduli (Meleard et al., 1997; Niggemann et al., 1995). Gel phase membranes, on the other hand, are dominated by surface rigidity and as a result finite tensions are required to induce shape deformations (Evans and Needham, 1987). Two-phase vesicles show behavior that is intermediate between purely L_α and purely gel phase membranes. At low gel fractions, the membrane is primarily fluid and appears to respond to tension elastically. The only exception is when large domains become trapped at the tip of the micropipette, similar to what is seen in Fig. 11, bottom left and right. In this situation, the gel resists the sharp bending deformation that would result from entering the micropipette tip. The network momentarily supports the increasing stress so there is no change in vesicle projection length. This continues until the network plastically deforms and enters the tip. This phenomenon is manifested in the stress/strain data as the ''steps'' on otherwise linear curves as seen in Fig. 3 *B*. Vesicles with higher gel fractions, i.e., farther away from the coexistence line, exhibit a more extensive domain network and stress/strain curves become increasingly nonlinear. Fig. 7 shows that curves begin to approach the behavior seen in fully gel-phase membranes (Evans and Needham, 1987) such as a finite tension needed to initially aspirate the membrane (*section of curve marked 1*) and marked hysteresis on tension reduction (marked in figure by 2 and 4). Again, it must be emphasized that it is only because the domains are present as an extended network rather than small disconnected bodies that relatively small gel fractions can cause the observed changes in membrane mechanical properties.

Although the physical appearance of coexistence vesicles and the shapes of their stress/strain curves are explainable, one important question remains—why do we measure a 20–40% critical tension reduction for these vesicles? Evans and Needham have shown a fivefold *increase* in the tension required to rupture single-component lipid vesicles when they cross from the pure L_α into the pure gel state (Evans and Needham, 1987). Because in our system this stronger gel phase is present as a network, one might intuitively predict

that a reinforcing phenomenon would strengthen two-phase vesicles, especially at high gel domain fraction. However, our data indicate that this is not the case.

The fact that the rupture tension of a two-phase membrane is closer to that of a pure L_α vesicle than a (tougher) pure gel-phase vesicle suggests that the failure is occurring in the weaker L_α phase. Thus the data suggest that the L_α phase in coexistent vesicles fails before homogeneous L_α vesicles. Note that Fig. 5 shows that the lipid composition in the L_α phase does not affect τ_c, indicating that the depletion of DPPC from the phase-separated L_α phase does not contribute to the critical tension reduction.

We believe there are two likely sources of this apparent mechanical reduction in stability. First, the use of Eq. 2 to calculate membrane tension assumes the tension to be uniform at all points on the membrane. However, because two-phase membranes are a composite of materials with different mechanical properties, this is not necessarily the case. As shown in Eq. 1, tension is inversely related to the local radius of curvature. Therefore, the assumption of uniform tension is valid only if the vesicle adopts a perfectly spherical shape. (Effects of the pipette tip have been discussed elsewhere (Kwok and Evans, 1981).) Because they are homogeneous and cannot support a surface shear, this criterion is met in the aspiration of single-phase L_α membranes. This, however, may not necessarily be the case for L_α-gel coexistence vesicles. Although Fig. 6 shows that two-phase membranes appear to adopt an overall spherical shape once they are pressurized, there may be local regions with nonspherical topology. This would be due to both the solid-like properties of the gel phase and the lower elastic modulus of the L_α phase (as an illustration, imagine the two different radii of curvature for an inflated balloon stitched together from a stiff and a compliant elastomer). If an L_α region of the membrane had a local radius of curvature smaller than the overall vesicle, it would actually be under a higher tension than predicted by Eq. 2. Therefore the properties of the L_α phase in two-phase vesicles might be identical to single-phase L_α vesicles and the apparent τ_c reduction we measure is simply due to nonuniform radii of curvature effects. Note that if this were the case, our measured reduction in critical tension would not constitute an artifact. Regardless of the complications in calculating exact local values of tension, our data still indicate that two-phase membranes can support a smaller load before failure and can thus be considered weaker than their single L_α phase counterparts.

The second possible source of stability reduction is based on the large lateral density fluctuations experienced by lipids located at the domain interface (Clerc and Thompson, 1995). Because membranes fail through the formation of unstable defects (Deryagin and Gutop, 1962), fluctuations at the domain boundary may reduce the strength of the membrane by serving as sources for defect nucleation. Studies on the mechanical properties of two-phase vesicles exhibiting less extended or less mechanically dissimilar domains may be able to differentiate between these two possibilities.

CONCLUSIONS

In this work, we have examined the mechanical properties of POPC/DPPC lipid vesicles made at temperatures both above and within the L_α-gel coexistence region. When in the L_α phase, we find that the mechanical parameters K and τ_c are unaffected by composition but both decrease with temperature. These effects are key whenever membranes may face large temperature shifts, including biological systems that are not temperature regulated (i.e., bacteria) and vesicles for use in engineering applications (for example, during processing).

Marked differences in membrane material properties are found in the two-phase coexistence regime. Vesicles no longer behave as elastic materials and we measure a 20–40% decrease in the tension required to rupture. These observations are partly explained through fluorescent imaging of the domains in the POPC/DPPC mixtures. We show that domains with gel-like characteristics form a network in the vesicle, prompting changes in vesicle mechanical properties. An important point unanswered by this work is identifying the cause of the reduction in mechanical stability for two-phase lipid membranes. As many cellular membranes are believed to demonstrate lipid domain formation in vivo, these findings could have important biological implications.

We would like to thank Dr. Z. Suo and Dr. D. Srolovitz for helpful discussions.

We also gratefully acknowledge the National Science Foundation (CTS-9907687) and Rhodia (Fellowship to S.D.S.) for their financial support.

REFERENCES

Angelova, M. I., and D. S. Dimitrov. 1987. Swelling of charged lipids and formation of liposomes on electrode surfaces. *Molecular Crystals and Liquid Crystals.* 152:89–104.

Bagatolli, L. A., and E. Gratton. 2000a. A correlation between lipid domain shape and binary phospholipid mixture composition in free standing bilayers: a two-photon fluorescence microscopy study. *Biophys. J.* 79:434–447.

Bagatolli, L. A., and E. Gratton. 2000b. Two photon fluorescence microscopy of coexisting lipid domains in giant unilamellar vesicles of binary phospholipid mixtures. *Biophys. J.* 78:290–305.

Brown, D. A., and E. London. 1998. Functions of lipid rafts in biological membranes. *Annu. Rev. Cell Dev. Biol.* 14:111–136.

Clerc, S. G., and T. E. Thompson. 1995. Permeability of dimyristoyl phosphatidylcholine/dipalmitoyl phosphatidylcholine bilayer-membranes with coexisting gel and liquid-crystalline phases. *Biophys. J.* 68: 2333–2341.

Curatolo, W., B. Sears, and L. J. Neuringer. 1985. A calorimetry and deuterium NMR study of mixed model membranes of 1-palmitoyl-2-oleylphosphatidylcholine and saturated phosphatidylcholines. *Biochim. Biophys. Acta.* 817:261–270.

de Almeida, R., L. Loura, A. Fedorov, and M. Prieto. 2002. Nonequilibrium phenomena in the phase separation of a two- component lipid bilayer. *Biophys. J.* 82:823–834.

Deryagin, B., and Y. Gutop. 1962. Theory of the breakdown (rupture) of free films. *Kolloidn. Zh.* 24:370–374.

Dufrene, Y. F., W. R. Barger, J. B. D. Green, and G. U. Lee. 1997. Nanometer-scale surface properties of mixed phospholipid monolayers and bilayers. *Langmuir.* 13:4779–4784.

Evans, E., and F. Ludwig. 2000. Dynamic strengths of molecular anchoring and material cohesion in fluid biomembranes. *Journal of Physics-Condensed Matter.* 12:A315–A320.

Evans, E., and D. Needham. 1987. Physical properties of surfactant membranes: thermal transitions, elasticity, rigidity, cohesion, and colliodal interactions. *J. Phys. Chem.* 91:4219–4228.

Evans, E., W. Rawicz, and A. F. Hofman. 1995. Lipid bilayer expansion and mechanical disruption in solutions of water-soluble bile acid. *In* Bile Acids in Gastroenterology Basic and Clinical Advances. A. F. Hofmann, G. Paumgartner, and A. Stiehl, editors. Kluwer Academic, Boston.

Evans, E., and R. Skalak. 1980. Mechanics and Thermodynamics of Biomembranes. CRC Press, Boca Raton.

Fernandez-Puente, L., I. Bivas, M. D. Mitov, and P. Meleard. 1994. Temperature and chain-length effects on bending elasticity of phosphatidylcholine bilayers. *Europhysics Letters.* 28:181–186.

Haverstick, D. M., and M. Glaser. 1987. Visualization of Ca2+-induced phospholipid domains. *Proc. Natl. Acad. Sci. USA.* 84:4475–4479.

Hui, S. W. 1981. Geometry of phase-separated domains in phospholipid-bilayers by diffraction-contrast electron-microscopy. *Biophys. J.* 34:383–395.

Israelachvili, J. N., S. Marcelja, and R. G. Horn. 1980. Physical principles of membrane organization. *Q. Rev. Biophys.* 13:121–200.

Jasper, J., and J. Duncan. 1967. Temperature-interfacial tension studies of some 1-alkenes against water. *Journal of Chemical and Engineering Data.* 12:257–259.

Jorgensen, K., A. Klinger, and R. L. Biltonen. 2000. Nonequilibrium lipid domain growth in the gel-fluid two-phase region of a DC16PC-DC22PC lipid mixture investigated by Monte Carlo computer simulation, FT-IR, and fluorescence spectroscopy. *Journal of Physical Chemistry B.* 104:11763–11773.

Jorgensen, K., M. M. Sperotto, O. G. Mouritsen, J. H. Ipsen, and M. J. Zuckermann. 1993. Phase-equilibria and local-structure in binary lipid bilayers. *Biochim. Biophys. Acta.* 1152:135–145.

Kates, M. 1993. Membrane-lipids of extreme halophiles - biosynthesis, function and evolutionary significance. *Experientia.* 49:1027–1036.

Korlach, J., P. Schwille, W. Webb, and G. Feigenson. 1999. Characterization of lipid bilayer phases by confocal microscopy and fluorescence correlation spectroscopy. *Proc. Natl. Acad. Sci. USA.* 96:8461–8466.

Kwok, R., and E. Evans. 1981. Thermoelasticity of large lecithin bilayer vesicles. *Biophys. J.* 35:637–652.

Longo, M., A. Waring, and D. Hammer. 1997. Interaction of the influenza hemagglutinin fusion peptide with lipid bilayers: area expansion and permeation. *Biophys. J.* 73:1430–1439.

Meleard, P., C. Gerbeaud, T. Pott, L. Fernandez-Puente, I. Bivas, M. D. Mitov, J. Dufourcq, and P. Bothorel. 1997. Bending elasticities of model membranes: influences of temperature and sterol content. *Biophys. J.* 72:2616–2629.

Mendelsohn, R., G. L. Liang, H. L. Strauss, and R. G. Snyder. 1995. IR spectroscopic determination of gel state miscibility in long-chain phosphatidylcholine mixtures. *Biophys. J.* 69:1987–1998.

Mou, J. X., J. Yang, and Z. F. Shao. 1995. Atomic-force microscopy of cholera-toxin B-oligomers bound to bilayers of biologically relevant lipids. *J. Mol. Biol.* 248:507–512.

Murga, M., D. Bernik, G. de Valdez, and A. Disalvo. 1999. Permeability and stability properties of membranes formed by lipids extracted from Lactobacillus Acidophilus grown at different temperatures. *Arch. Biochem. Biophys.* 364:115–121.

Needham, D., and E. Evans. 1988. Structure and mechanical properties of giant lipid (DMPC) vesicle bilayers from 20 degrees C below to 10 degrees C above the liquid crystral-crystalline phase transition at 24 degrees C. *Biochemistry.* 27:8261–8269.

Needham, D., and R. Nunn. 1990. Elastic deformation and failure of lipid bilayer membranes containing cholesterol. *Biophys. J.* 58:997–1009.

Needham, D., and D. Zhelev. 1995. Lysolipid exchange with lipid vesicle membranes. *Ann. Biomed. Eng.* 23:287–298.

Niggemann, G., M. Kummrow, and W. Helfrich. 1995. The bending rigidity of phosphatidylcholine bilayers - dependences on experimental-method, sample cell sealing and temperature. *Journal de Physique I I.* 5:413–425.

Olbrich, K., W. Rawicz, D. Needham, and E. Evans. 2000. Water permeability and mechanical strength of polyunsaturated lipid bilayers. *Biophys. J.* 79:321–327.

Rawicz, W., K. Olbrich, T. McIntosh, D. Needham, and E. Evans. 2000. Effect of chain length and unsaturation on elasticity of lipid bilayers. *Biophys. J.* 79:328–339.

Rodgers, W., and M. Glaser. 1991. Characterization of lipid domains in erythrocyte-membranes. *Proc. Natl. Acad. Sci. USA.* 88:1364–1368.

Sankaram, M. B., D. Marsh, and T. E. Thompson. 1992. Determination of fluid and gel domain sizes in two-component, two-phase lipid bilayers. An electron-spin-resonance spin label study. *Biophys. J.* 63:340–349.

Schroeder, R., E. London, and D. Brown. 1994. Interactions between saturated acyl chains confer detergent resistance on lipids and Glycosylphosphatidylinositol (Gpi)-anchored proteins: Gpi-anchored proteins in liposomes and cells show similar behavior. *Proc. Natl. Acad. Sci. USA.* 91:12130–12134.

Shoemaker, S., and T. K. Vanderlick. 2002a. Intramembrane electrostatic interactions destabilize lipid membranes. *Biophys. J.* 83:2007–2014.

Shoemaker, S., and T. K. Vanderlick. 2002b. Stress-induced leakage from phospholid vesicles: effect of membrane composition. *Industrial & Engineering Chemistry Research.* 41:324–329.

Silvius, J. 1982. Lipid-Protein Interactions. John Wiley & Sons, New York.

Vaz, W., R. Clegg, and D. Hallmann. 1985. Translational diffusion of lipids in liquid-crystalline phase phosphatidylcholine multibilayers. A comparison of experiment with theory. *Biochemistry.* 24:781–786.

Veldhuizen, R., K. Nag, S. Orgeig, and F. Possmayer. 1998. The role of lipids in pulmonary surfactant. *Biochim. Biophys. Acta.* 1408:90–108.

Washburn, E., editor. 1927. International Critical Tables. McGraw Hill, New York.

Yeagle, P. 1992. The Structure of Biological Membranes. CRC Press, Boca Raton.

Zhelev, D., and D. Needham. 1993. Tension-stabilized pores in giant vesicles: determination of pore size and pore line tension. *Biochim. Biophys. Acta.* 1147:89–104.